Current Applied Physics 13 (2013) 717–724

Contents lists available at SciVerse ScienceDirect

Current Applied Physics

journal homepage: www.elsevier.com/locate/cap

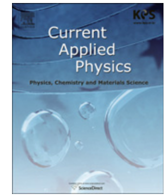

The effect of differently sized Ag catalysts on the fabrication of a silicon nanowire array using Ag-assisted electroless etching

Ai-Huei Chiou [a], Tse-Chang Chien [a], Ching-Kuei Su [a], Jheng-Fong Lin [a], Chun-Yao Hsu [b,*]

[a] *Department of Mechanical Engineering, National Chiao Tung University, Hsinchu, Taiwan, ROC*
[b] *Department of Mechanical Engineering, Lunghwa University of Science and Technology, Taiwan, ROC*

A R T I C L E I N F O

Article history:
Received 10 July 2012
Received in revised form
28 October 2012
Accepted 20 November 2012
Available online 30 November 2012

Keywords:
Ag catalysts
Silicon nanowires array
Electroless metal deposition

A B S T R A C T

A simple and low cost method to generate single-crystalline, well-aligned silicon nanowires (SiNWs) of large area, using Ag-assisted electroless etching, is presented and the effect of differently sized Ag catalysts on the fabrication of SiNWs arrays is investigated. The experimental results show that the size of the Ag catalysts can be controlled by adjusting the pre-deposition time in the $AgNO_3$/HF solution. The optimum pre-deposition time for the fabrication of a SiNWs array is 3 min (about 162.04 ± 38.53 nm Ag catalyst size). Ag catalysts with smaller sizes were formed in a shorter pre-deposition time (0.5 min), which induced the formation of silicon holes. In contrast, a large amount of Ag dendrites were formed on the silicon substrate, after a longer pre-deposition time (4 min). The existence of these Ag dendrites is disadvantageous to the fabrication of SiNWs. Therefore, a proper pre-deposition time for the Ag catalyst is beneficial to the formation of SiNWs.

SiNWs were synthesized in the H_2O_2/HF solution system for different periods of time, using Ag-assisted electroless etching (pre-deposition of the Ag catalyst for 3 min). The length of the SiNWs increases linearly with immersion time. From TEM, SAED and HRTEM analysis, the axial orientation of the SiNWs is identified to be along the [001] direction, which is the same as that of the initial Si wafer. The use of HF may induce Si–H_x bonds onto the SiNW array surface. Overall, the Ag-assisted electroless etching technique has advantages, such as low temperature, operation without the need for high energy and the lack of a need for catalysts or dopants.

© 2012 Elsevier B.V. All rights reserved.

1. Introduction

One-dimensional nanowires, such as Si [1], Ge [2], InP [3], GaAs [4] and SnO_2 [5], have been widely studied, since the discovery of carbon nanotubes in 1991. Of the many one-dimensional (1D) materials, silicon nanowires (SiNWs) are perhaps the most important. Silicon has found widespread applications as a semiconducting material and its microelectronic technology is one of the greatest successes of the 20th century. Papers have been published which detail the use of SiNWs in applications such as biological and chemical sensors [6–9]. Therefore, the importance of SiNWs to the semiconductor, optoelectronics, biomedical, or energy industries cannot be overstated. There are many methods for the synthesis of 1D SiNW arrays, including the vapor–liquid–solid growth mechanism [10], the solution-liquid–solid growth mechanism [11], the gas–solid growth mechanism [12], laser-assisted catalytic growth [13], template-based synthetic methods [14], physical vapor deposition [15], chemical vapor deposition [16] and oxide-assisted nucleation [17]. However, some methods, such as catalytic growth using the vapor liquid solid method and metal organic-chemical vapor deposition, are expensive, energy-consuming processes that require extreme conditions.

Recently, Peng et al. [18–28] demonstrated wall-aligned SiNW arrays, fabricated using facile assisted-metal etching. This method of fabricating a SiNW array has many advantages, such as low cost and large surface area. It also allows the control of conductivity, which facilitates applications in electronic devices such as field-effect transistors, lithium ion batteries and electrochemical biosensors, but the repeatable and controllable preparation of SiNW arrays from a substrate, with defined type, orientation, size, doping level and improved conductivity still poses a challenge. Many catalysts, such as Ag, Au, Ni, Ti and Fe, are used to prepare SiNWs. However, few studies have considered the effect of Ag catalysts in the fabrication process for silicon SiNW arrays. This study aims to provide a simple method for the generation of SiNWs of large area, directly synthesized on p-type (100) silicon wafer. It also examines the effect of differently sized Ag catalysts on the fabrication of SiNW arrays.

* Corresponding author. Fax: +886 2 82094845.
E-mail address: cyhsu@mail.lhu.edu.tw (C.-Y. Hsu).

1567-1739/$ – see front matter © 2012 Elsevier B.V. All rights reserved.
http://dx.doi.org/10.1016/j.cap.2012.11.011

2. Experimental procedures

The Ag catalyst for the fabrication of a silicon nanowire array by Ag-assisted electroless etching uses a sequence of two solutions; solution I is based on $AgNO_3$/HF and solution II is based on H_2O_2/HF. Firstly, 6-inch p-type (100) oriented silicon wafer substrates with a resistivity of 15–25 Ω-cm are used in this study. In order to remove chemical impurities and particles, the wafers were cleaned using a standard Radio Corporation of American cleaning process [29]. In this procedure, the silicon substrates were cut into squares and washed with DI water. The samples were then immersed in an $AgNO_3$/HF system at 50 °C, for times of 0.5–4 min, to synthesize Ag catalysts. After synthesis of the Ag catalysts, SiNWs were synthesized, using Ag-assisted electroless etching in a H_2O_2:HF = 0.5:4.6 M solution at 50 °C, for different periods of time. The SiNW arrays were coated with the residual Ag of the prepared SiNW arrays, so the as-prepared samples were dipped in 30% HNO_3 solution. Finally, the SiNW arrays were immersed in the 10% HF solution, to remove the oxide layer on the SiNW arrays, and then washed with deionized water and dried by blowing with nitrogen. A schematic illustration of the Ag catalyst for the fabrication of a silicon nanowire array using Ag-assisted electroless etching is shown in Fig. 1.

The surface morphology of the Ag catalysts was determined using an atomic force microscope (AFM, NT-MDT Solver P47). The surface morphology of the SiNWs was investigated using field-emission scanning electron microscopy (FE-SEM, Hitachi S-4000) and transmission electron microscopy (TEM, JEM-2010F). The crystalline structure of the SiNWs was determined using X-ray diffraction (Rigaku-2000 X-ray Generator.), using Cu Kα radiation

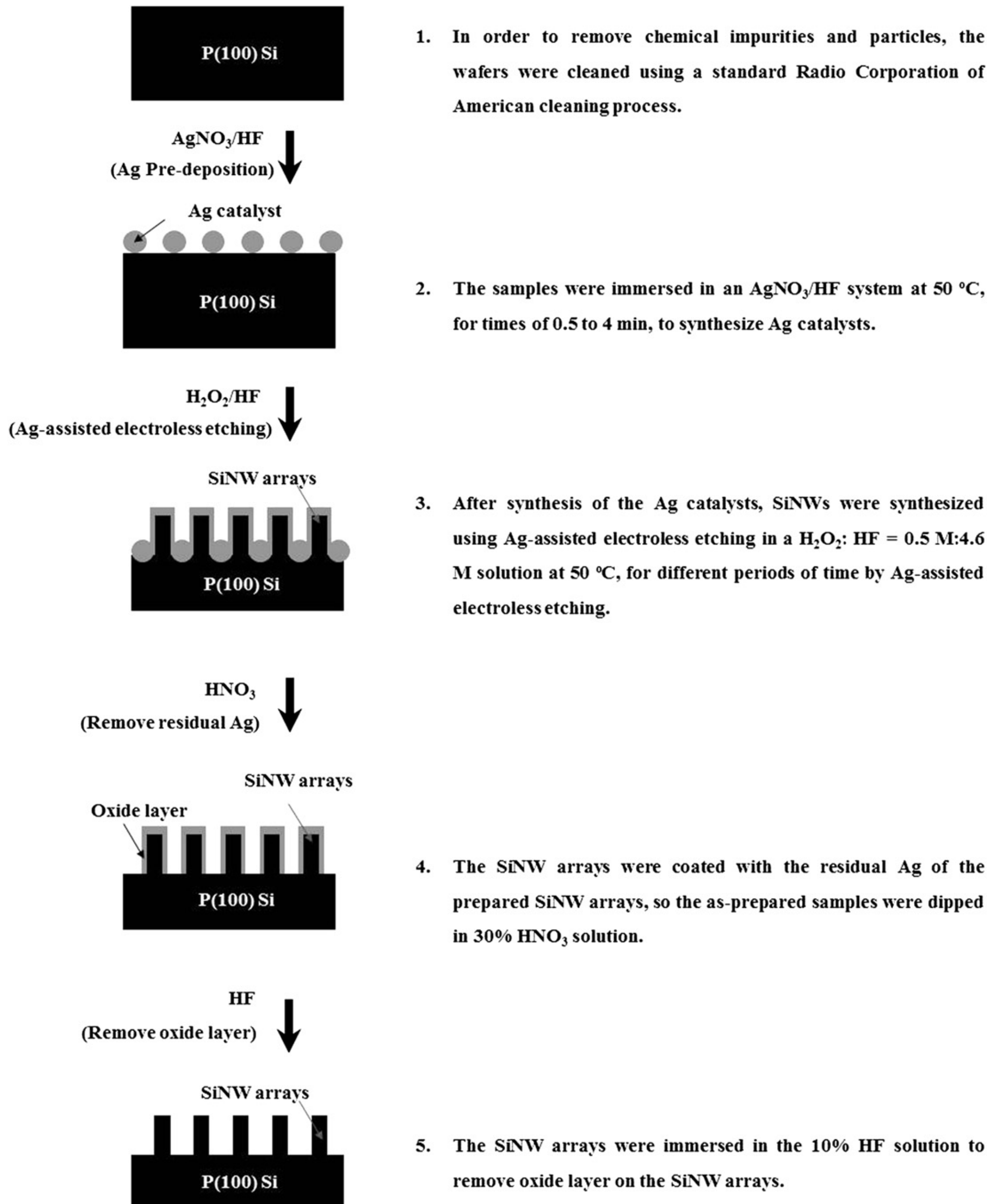

Fig. 1. Schematic illustration of the Ag-assisted electroless etching using a sequence of two solutions; solution I is based on $AgNO_3$/HF and solution II is based on H_2O_2/HF.

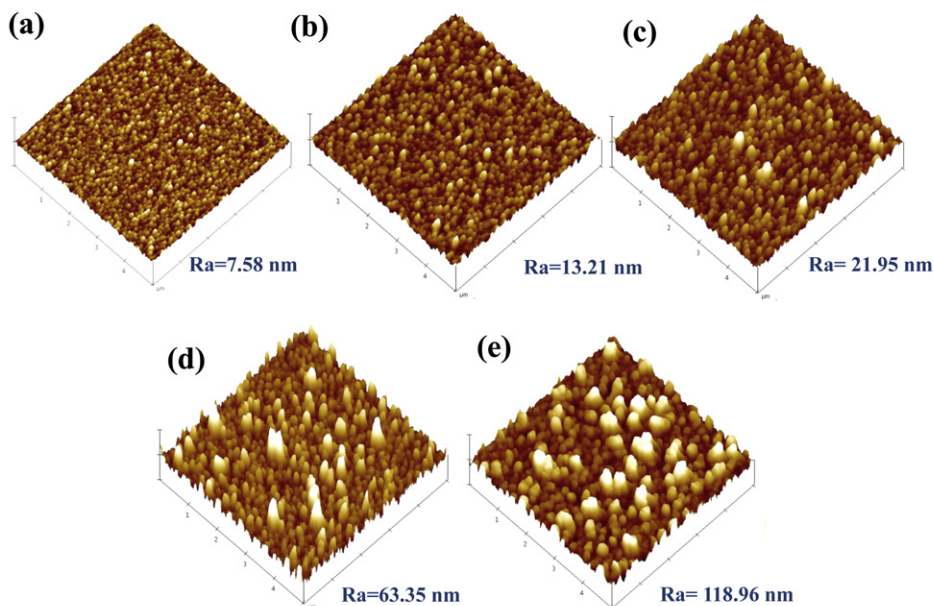

Fig. 2. AFM image and surface roughness (Ra) of Ag nanoparticles with a pre-deposition of (a) 0.5 min, (b) 1 min, (c) 2 min, (d) 3 min and (e) 4 min, at a concentration ratio of 0.01:4.6 M for $AgNO_3$/HF at 50 °C, (Ra: center line average roughness, Ra).

with an angle of incidence of 1°. A water contact angle system (WCA, FACE CA-VP150) was also used to analyze the hydrophilic and the hydrophobic nature of the SiNW arrays. Fourier transform infrared spectroscopy (FTIR, ASTeX PDS-17) was used to analyze the chemical composition.

3. Results and discussion

3.1. Characteristic analysis of the Ag catalysts

One of the key problems for the chemical growth of SiNWs is the synthesis of Ag catalysts, obtained by the pre-deposition of $AgNO_3$/HF solution. It has been reported that the nature of the SiNW arrays produced depends on synthesis parameters, such as the reaction temperature, catalyst composition and reaction time [30]. Therefore, the effect of different sizes of Ag catalyst on the fabrication of SiNW arrays is examined. In order to investigate the transformation of the Ag catalyst into nanoparticles, different pre-deposition times were used. Fig. 2 shows the AFM image and surface roughness (Ra)

Table 1
Surface roughness and grain size of Ag nanoparticles for different pre-deposition time, at a concentration ratio of 0.01:4.6 M for $AgNO_3$/HF, at 50 °C.

Samples	Roughness (Ra)	Grain size (nm)
0.5 min	8.637 ± 4.27	Unobvious
1 min	13.21 ± 1.50	117.78 ± 20.38
2 min	22.04 ± 1.98	156.8 ± 34.60
3 min	63.35 ± 4.04	162.04 ± 38.53
4 min	118.96 ± 10.29	202.08 ± 22.75

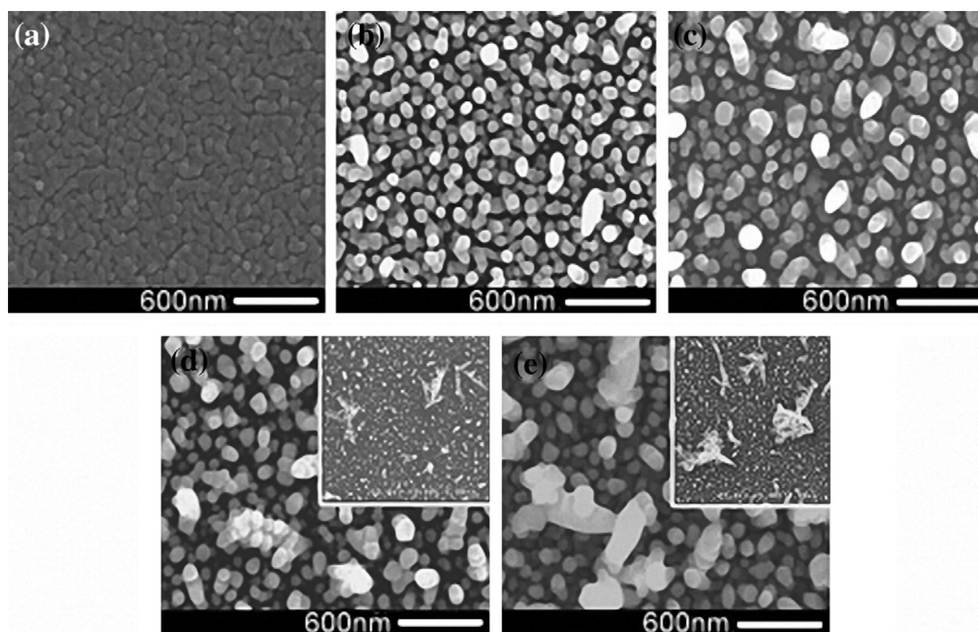

Fig. 3. SEM image of Ag nanoparticles deposited for (a) 0.5 min, (b) 1 min, (c) 2 min, (d) 3 min and (e) 4 min, at a concentration ratio of 0.01:4.6 M for $AgNO_3$/HF, at 50 °C.

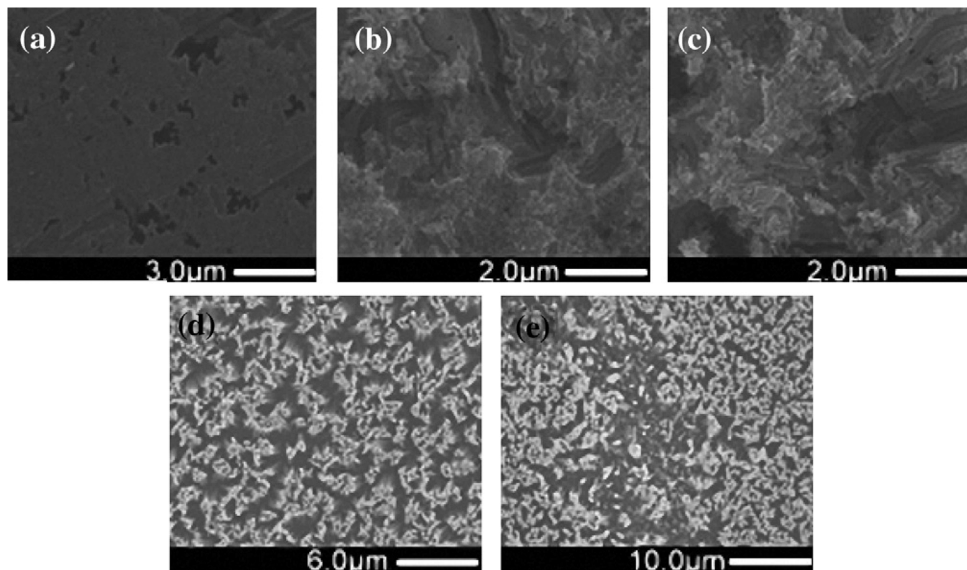

Fig. 4. SEM image of SiNW arrays with different Ag catalysts corresponding to Fig. 3, at a concentration ratio of 0.5:4.6 M for H_2O_2/HF, for 45 min at 50 °C.

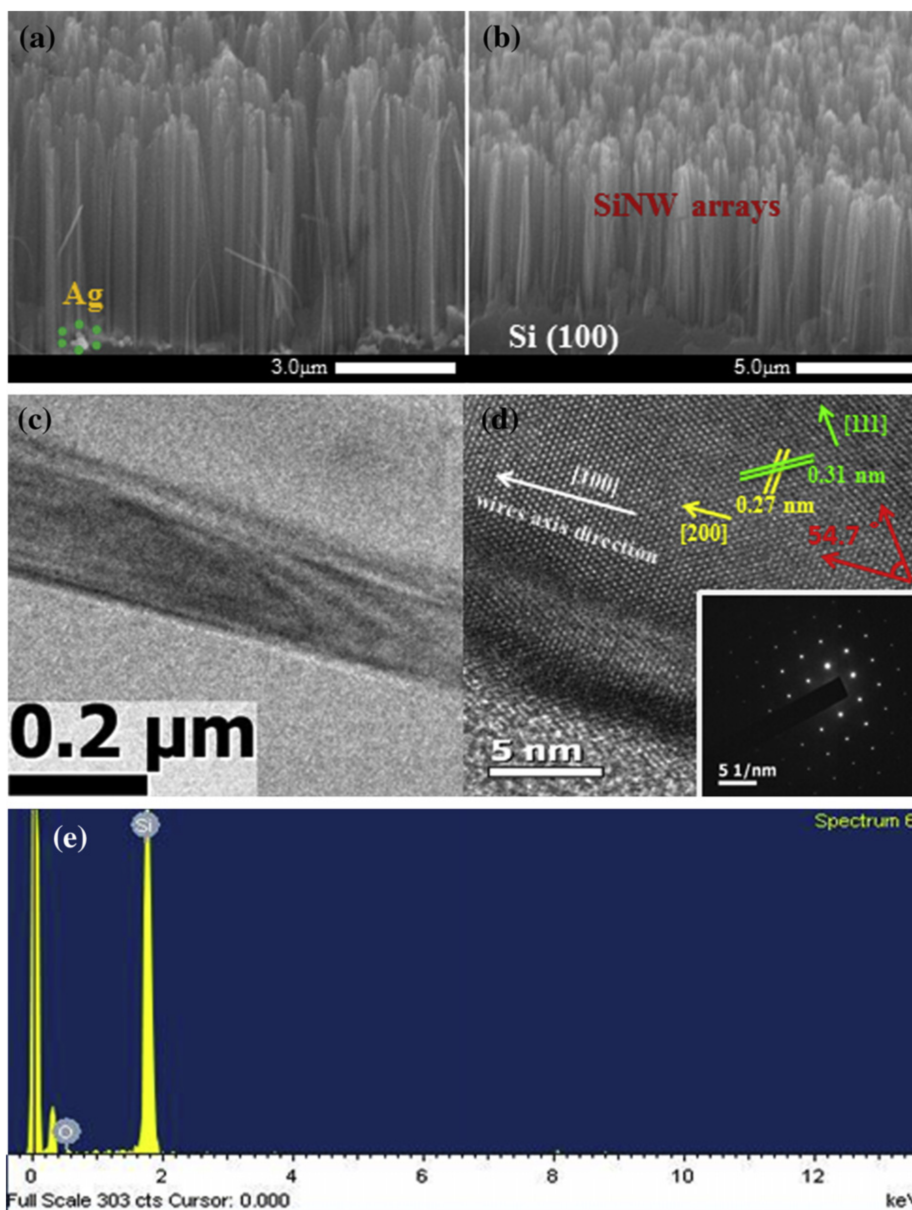

Fig. 5. Morphology and elemental analysis of SiNW arrays, without HNO_3 treatment (no removal of Ag particles), and with HNO_3 treatment (Ag particles remove).

of the high-density Ag catalysts prepared on silicon substrates in $AgNO_3$/HF solution, over various times. The results obtained from AFM show the Ag catalysts prepared on silicon substrates in $AgNO_3$/HF solution depend on pre-deposition time. In fact, it can be seen that a longer pre-deposition time results in denser Ag catalyst nanoparticles and higher surface roughness. The pre-deposition time is longer, the Ag particles and tree-like Ag dendrites become more numerous (Fig. 2(e)). If the pre-deposition time is longer, the particles impact with each other and agglomerate, because of Brownian motion [31].

Fig. 3 shows the SEM image of an Ag film on a sample. The number of tree-like Ag dendrites increases as the pre-deposition time increases to 3 or 4 min. For a deposition time of 0.5 min, the size of the Ag catalysts is small, with a highly dense distribution (see Fig. 3(a)). However, an increase in large amounts of Ag dendrite is observed as the pre-deposition time is increased. This occurs because the Ag catalyst changes from a particle shape to a cluster or dendrite structure, as pre-deposition time increases, so the structural uniformity of the Ag catalyst gradually deteriorates and the roughness increases.

The roughness and grain size of the Ag catalysts particles increases as pre-deposition time increases (see Table 1). For a shorter time, the particle size of the Ag catalysts is small. For a long time, the particle sizes of the Ag catalysts are large. This result indicates that increasing the pre-deposition time for $AgNO_3$ encourages the growth of Ag catalysts and leads to an increase in particle size (see Fig. 3). Fig. 3(e) shows that the Ag dendrites ratio is increased for the 4 min sample, using aqueous HF solution containing $AgNO_3$. The increase in the Ag dendrites ratio is probably due to over pre-deposition with aqueous HF solution containing $AgNO_3$. These results agree with those already reported [32].

3.2. *Characteristic analysis of the SiNW arrays*

In order to understand the effect of different sizes of Ag particles on SiNW arrays, Fig. 4 shows the formation of a SiNW array in the H_2O_2/HF etching system, at 50 °C for 45 min, with different sizes of Ag particles. When the pre-deposition time is too short (0.5 min), the Ag particles are denser and a SiNW array cannot be synthesized. Indicate that smaller and more dispersed Ag catalysts are formed for a shorter pre-deposition time, which induces the formation of a large amount of silicon holes, as shown in Fig. 4 (a) and (b). Fig. 4 (c) and (d) displays a plan view SEM image of a p-Si (1 0 0) sample which was subjected to Ag-assisted electroless etching in H_2O_2/HF solution for 45 min at 50 °C. It shows that the surface is microstructured with pillar-like structures and density of macropores. Beside, when the pre-deposition time is longer, many Ag dendrites are fabricated and the spacing becomes greater. However, a large amount of Ag dendrites is formed on the silicon substrate over a longer pre-deposition time (4 min), the existence of these Ag dendrites is disadvantageous to the fabrication of SiNW arrays, as shown in Fig. 4(e). A proper pre-deposition time (3 min) for the Ag catalyst is beneficial to the formation of SiNWs. It can be seen from these results that optimum values for the parameters used for the fabrication of SiNW arrays are necessary to ensure a perfect chemical etching process.

Fig. 5 shows the morphology and elemental analysis of the SiNW arrays, without HNO_3 treatment (no removal of Ag particles, Fig. 5(a)), and with HNO_3 treatment (Ag particles remove, Fig. 5(b)). Further structural and crystallographic characterization of the SiNW array was performed using a combined TEM and EDX spectrum. Fig. 5(c) shows typical TEM images of as-synthesized SiNWs, with a width of approximately 90–150 nm. Fig. 5(d) shows the HRTEM

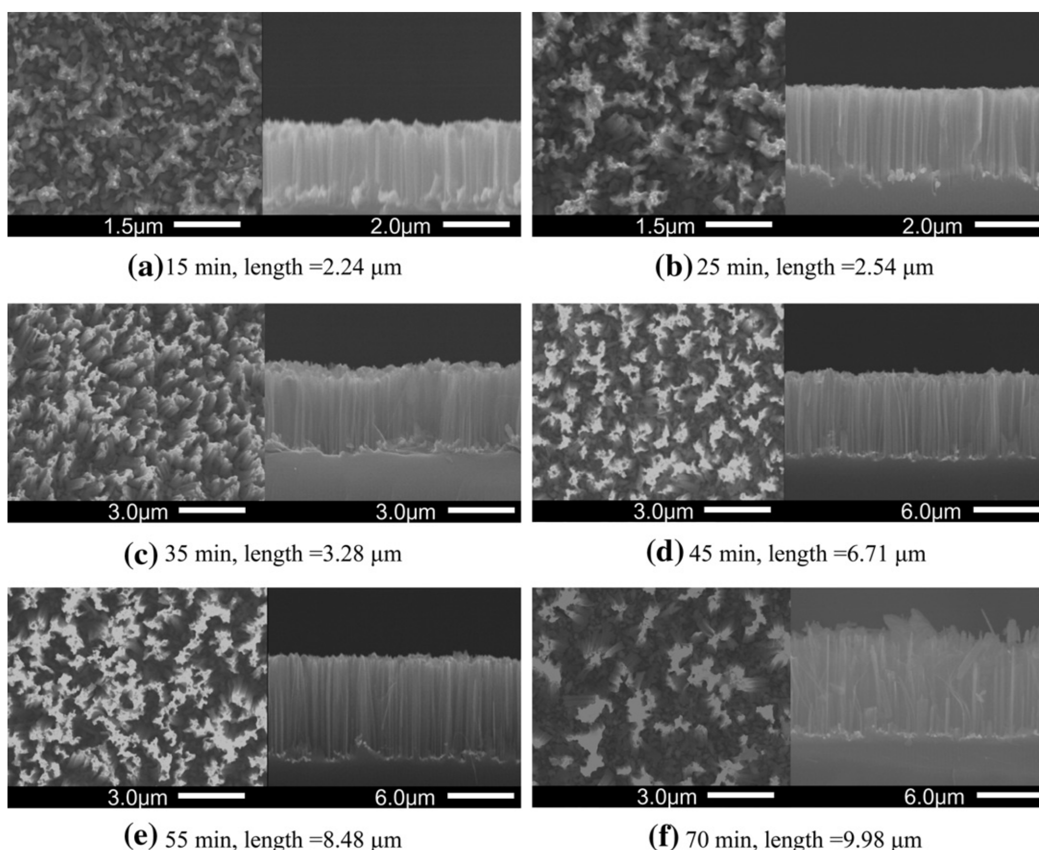

Fig. 6. SEM image of the top view and cross-section of the SiNW for different etching times, at a concentration ratio of 0.5:4.6 M for H_2O_2/HF at 50 °C.

images of the SiNWs. The corresponding axial directions, characterized by selected area electron diffraction (SAED) patterns, are shown in the inset. The corresponding SADE patterns show the [111] and [200] zone axes of silicon, respectively. This result indicates that the axial direction of the SiNW array is along the [100] direction, which is identical to the (100)-oriented orientation of the preferred p-type. SiNWs were characterized by SAED patterns, which indicate that the crystal is single crystalline. The EDX analysis verifies that the SiNWs are silicon and shows only one peak that is comparable to Si, after HNO_3 treatment, which indicates that the residual Ag nanoparticles are removed completely, as shown in Fig. 5(e).

Fig. 6 shows the side-view SEM images of the SiNW arrays prepared using (100)-oriented silicon substrates in etching solution, at 50 °C, with various etching times from 15 to 70 min. The SiNW arrays, which are straight and grow vertically on the silicon substrates, can be observed in the micrographs. The length of the SiNW array increases as etching time increases. Fig. 7 shows the lengths range from 2.24 to 10.03 μm, corresponding to Fig. 6. According to the dynamic theory, the linear relationship of the SiNW array can be adjusted by controlling the etching time for Ag-assisted electroless etching. The conglomeration at the tips of the SiNWs array also increases as etching time increases, because of the strong force or Van der Waals interaction [33]. Fig. 8 shows the X-ray diffraction spectrum for SiNW arrays, etching time 55 min, without HNO_3 treatment (no removal of Ag particles) and with HNO_3 treatment (Ag particles remove). Fig. 8(a), without HNO_3 treatment the SiNW array has diffraction peaks at 38.3°, 44.4°, 64.6° and 77.5°, which belong to the (111), (200), (220) and (311) Ag planes, respectively. After HNO_3 treatment, the peaks occur at 69.4° and belong to the (400) silicon planes (Fig. 8(b)). Literature [34] shows that the axial direction of the SiNW arrays has a preferred orientation of [100]. This result is consistent with the HRTEM image. Fig. 9 shows the XRD diffraction patterns for the SiNW arrays, under different etching time. It is clear that the (400) silicon diffraction peak, located at 2θ ~69.4°, is observed, shows the better crystallinity of the SiNW array in etching solution at 50 °C for 55 min (the diffraction peaks are sharper and more intense, Fig. 9(g)).

Water contact angle (WCA) analysis is sensitive to the chemical composition of the topmost molecular layer and is a relatively simple, inexpensive and popular technique for the characterization of material surfaces. A chemical band analysis was performed for the SINW arrays with and without HF treatment. After HF treatment, the sample surface can induce extremely hydrophobic functional groups. Fig. 10 shows WCA observation. Fig. 10(b) shows that the SiNW arrays without HF treatment have extremely hydrophilic features (contact angle of 4.1°). After HF treatment, the SiNW arrays become extremely hydrophobic (contact angle of 138.2°), as shown in Fig. 10(c). The use of HF treatment may induce Si–H_x bonds onto surface of the SiNW arrays, which can be confirmed by FTIR analysis, as shown in Fig. 11. The peak at 620 cm^{-1} is attributed to Si–Si rocking vibration. The SiNW arrays without HF treatment, the signals from Si–O bonds (peak at 1100–1250 cm^{-1}) are much stronger and other O–H bonds, as shown in Fig. 11(a). However, after HF treatment, the absorbance of the Si–O bonds is weaker, and Si–H_x asymmetric stretching mode bands at 2245 cm^{-1} are observed, the stronger Si–H_x signal reflects the fact that the surface is mainly terminated by Si–H_x bonds, as shown in Fig. 11(b). This result pointed out that the previous oxide layer was dissolved in the HF solution. The use of HF induces Si–H_x bonds

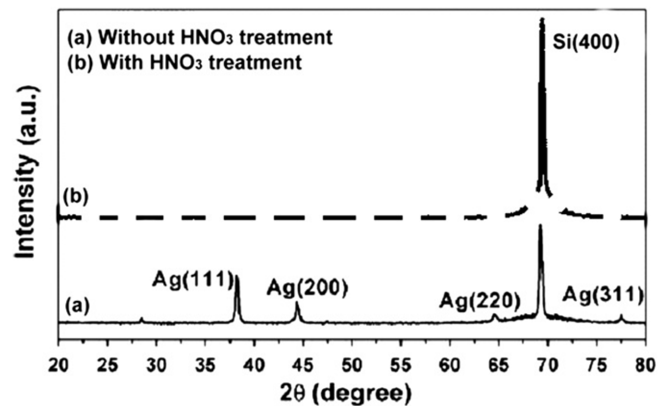

Fig. 8. X-ray diffraction spectrum for SiNW arrays, etching times 55 min: (a) without HNO_3 treatment (no removal of Ag particles), (b) with HNO_3 treatment (Ag particles remove).

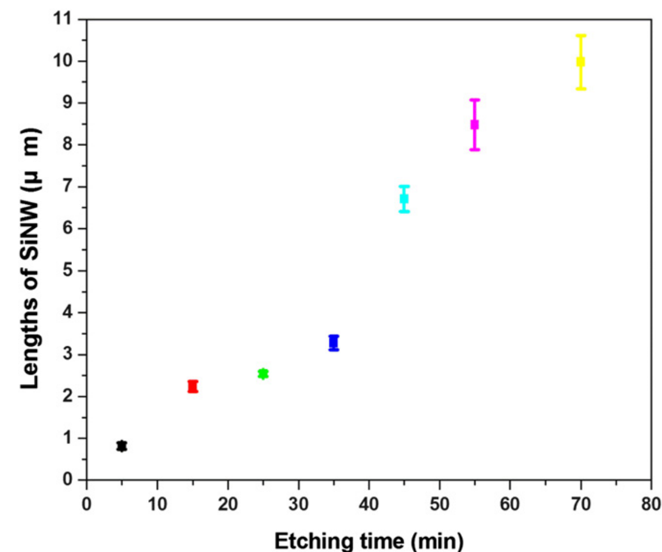

Fig. 7. The effect of etching time on the length of SiNW arrays corresponding to Fig. 6, at a concentration ratio of 0.5:4.6 M for H_2O_2/HF at 50 °C.

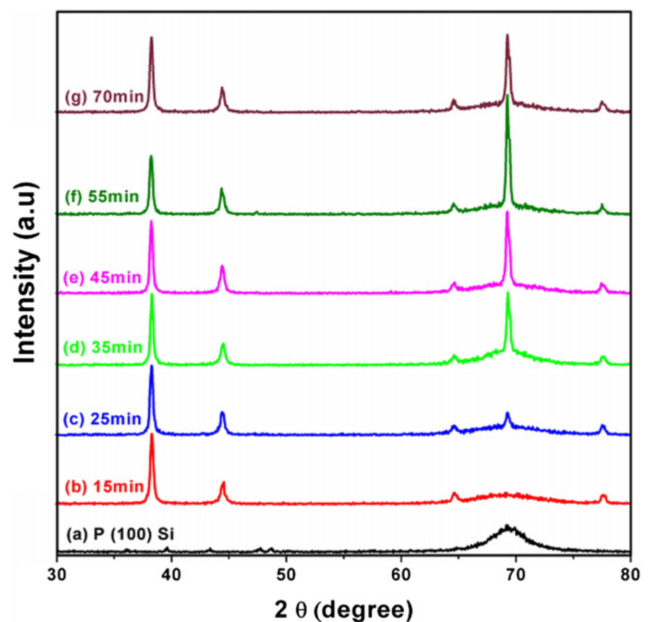

Fig. 9. Structural properties of SiNW arrays at a concentration ratio of 0.5:4.6 M for H_2O_2/HF, at 50 °C, corresponding to Fig. 6, with different etching time: (a) P-Si, (b) 15 min, b = unobvious (c) 25 min, b = 0.319, (d) 35 min, b = 0.301, (e) 45 min, b = 0.300, (f) 55 min, b = 0.298 and (g) 70 min, b = 0.333, (b: full width at half maximum, FWHM. No removal of Ag particles).

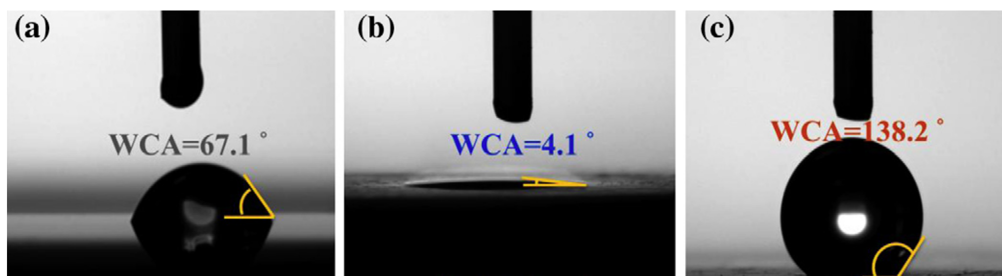

Fig. 10. WCA observation of (a) Si substrate, (b) SiNW arrays without HF treatment (hydrophilic) and (c) SiNW arrays with HF treatment (hydrophobic).

onto the SiNW arrays surface, which can be confirmed by WCA analysis (corresponding to Fig. 10(c)).

3.3. Reaction mechanism of Ag-assisted electroless etching

In this study, SiNW arrays were fabricated by a two-step process, using Ag catalysts in the H_2O_2/HF etching agent. The role of Ag film in SiNWs growth in the H_2O_2/HF solution is consistent with previous reports. In this case, AgNPs are oxidized by H_2O_2, initially producing Ag^+. Then, Ag^+ is reduced by electrons from the closest Si atoms, producing Si underneath the AgNPs. Meanwhile, HF dissolves SiO_2, leaving shallow pits underneath the AgNPs. As time progresses, the AgNPs subside and the pits are gradually formed.

As discussed previously, different chemical reactions dominate in the two different electroless chemical etching processes. A series of redox reactions in $AgNO_3$/HF solution are outlined in Eqs. (1)–(3):

$$Ag^+ + e^- \rightarrow Ag \quad (1)$$

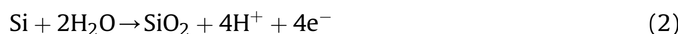

$$Si + 2H_2O \rightarrow SiO_2 + 4H^+ + 4e^- \quad (2)$$

$$SiO_2 + 6HF \rightarrow H_2SiF_6 + 2H_2O \quad (3)$$

The reaction in the H_2O_2/HF solution can be expressed as:

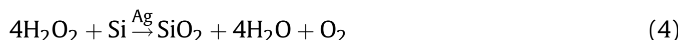

$$4H_2O_2 + Si \overset{Ag}{\rightarrow} SiO_2 + 4H_2O + O_2 \quad (4)$$

$$SiO_2 + 6HF \rightarrow H_2SiF_6 + 2H_2O \quad (5)$$

In the $AgNO_3$/HF solution, Ag^+ is abundant and oxidizes the exposed Si, producing SiO_2, which is then easily etched away by HF acid. The etching speed of the SiO_2 beneath AgNPs is relatively slow, so the Si underneath the Ag nanoparticles is preserved. However, in the H_2O_2/HF solution, Ag^+ is produced by the reduction of H_2O_2. Since this chemical reactivity is not high, Ag^+ mainly distributes close to the Ag film, so only Si underneath the Ag particles is prone to oxidation by Ag^+ and then etched away by HF acid. These results are in agreement with those already reported [35].

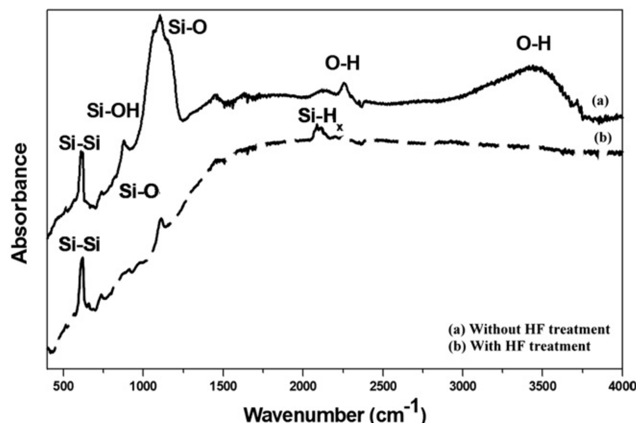

Fig. 11. Comparison of FTIR spectra, at a concentration ratio of 0.5:4.6 M for H_2O_2/HF, at 50 °C and 55 min: (a) SiNW arrays without HF treatment corresponding to Fig. 10(b) (hydrophilic), and (b) SiNW arrays with HF treatment corresponding to Fig. 10(c) (hydrophobic).

4. Conclusion

Synthesized single-crystalline, well-aligned, SiNW arrays of large area can be successfully produced on single crystal P (100) silicon wafer using a simple, low cost Ag-assisted electroless etching process. An optimally sized Ag catalyst for the fabrication of SiNW arrays requires a 3 min pre-deposition time. It can be seen that the optimization of the experimental parameters for the fabrication of SiNW arrays is important for the Ag-assisted electroless etching process used in this study.

SiNW arrays were synthesized in a H_2O_2/HF system, for different times, from 15 to 70 min, using Ag-assisted electroless etching (with pre-deposition of the Ag catalyst for 3 min). The results of this study show that the length of the SiNW arrays increases as the immersion time in the H_2O_2/HF system increases and that the SiNW arrays are bundled together, which appears to be typical for long SiNW arrays.

The axial orientation of the SiNWs was identified to be along the [001] direction, which is the same as that of the initial Si wafer. HF treatment was confirmed to be an effective precursor to the introduction of Si–H_x bonds onto the SiNW array surface, to enhance the hydrophobic nature. Overall, these results demonstrate that Ag-assisted electroless etching technique is an effective, reliable, low temperature method that does not require high energy.

References

[1] Y.L. Chueh, L.J. Chou, S.L. Cheng, J.H. He, W.W. Wu, L.J. Chen, Appl. Phys. Lett. 86 (2005) 133112.
[2] J.W. Dailey, J. Taraci, T. Clement, D.J. Smith, J. Drucker, S.T. Picraux, J. Appl. Phys. 96 (2004) 7556.
[3] S.D. Franceschi, J.A. van Dam, E.P.A.M. Bakkers, L.F. Feiner, L. Gurevich, L.P. Kouwenhoven, Appl. Phys. Lett. 83 (2003) 344.
[4] N. Panev, A.I. Persson, N. Sköld, L. Samuelson, Appl. Phys. Lett. 83 (2003) 2238.
[5] Z.R. Dai, J.L. Gole, J.D. Stout, Z.L. Wang, J. Phys. Chem. B 106 (2002) 1274.
[6] Y.F. Zhang, Y.H. Tang, N. Wang, D.P. Yu, C.S. Lee, I. Bello, S.T. Lee, Appl. Phys. Lett. 72 (1998) 1835.
[7] M.W. Shao, D.D.D. Ma, S.T. Lee, Eur. J. Inorg. Chem. 264 (2010).
[8] K.Q. Peng, S.T. Lee, Adv. Mater. 23 (2011) 198.
[9] P.R. Bandaru, P. Pichanusakorn, Semicond. Sci. Tech. 25 (2010) 024003.
[10] M. Haupt, A. Ladenburger, R. Sauer, K. Thonke, R. Glass, W. Roos, J.P. Spatz, H. Rauscher, S. Riethmüller, M. Möller, J. Appl. Phys. 93 (2003) 6252.
[11] T.J. Trentler, K.M. Hickman, S.C. Goel, A.M. Viano, P.C. Gibbons, W.E. Buhro, Science 270 (1995) 1791.
[12] X. Duan, C.M. Lieber, Adv. Mater. 12 (2000) 298.
[13] X. Duan, C.M. Lieber, J. Am. Chem. Soc. 122 (2000) 188.
[14] Y. Li, G.W. Meng, L.D. Zhang, F. Phillipp, Appl. Phys. Lett. 76 (2000) 2011.

[15] G. Gu, M. Burghard, G.T. Kim, S. Dusberg, P.W. Chiu, V. Krstic, S. Roth, W.Q. Han, J. Appl. Phys. 90 (2000) 5747.
[16] S.W. Kim, S. Fujita, S. Fujita, Appl. Phys. Lett. 86 (2005) 153119.
[17] N. Wang, Y.F. Zhang, Y.H. Tang, C.S. Lee, S.T. Lee, Appl. Phys. Lett. 73 (1998) 3902.
[18] K.Q. Peng, Y.J. Yan, S.P. Gao, Z. Jing, Adv. Funct. Mater. 13 (2003) 127.
[19] K. Peng, J. Zhu, J. Electroanal. Chem. 558 (2003) 35.
[20] F.M. Kolb, H. Hofmeister, R. Scholz, M. Zacharias, U. Gosele, D.D. Ma, S.T. Lee, J. Electrochem. Soc. 151 (2004) G472.
[21] K.Q. Peng, J.S. Jie, W.J. Zhang, S.T. Lee, Appl. Phys. Lett. 93 (2008) 033105.
[22] K.Q. Peng, A.J. Lu, R.Q. Zhang, S.T. Lee, Adv. Funct. Mater. 18 (2008) 3026.
[23] K.Q. Peng, X. Wang, S.T. Lee, Appl. Phys. Lett. 92 (2008) 163103.
[24] M.L. Zhang, K.Q. Peng, X. Fan, J.S. Jie, R.Q. Zhang, S.T. Lee, N.B. Wong, J. Phys. Chem. C 112 (2008) 4444.
[25] M.L. Zhang, C.Q. Yi, X. Fan, K.Q. Peng, N.B. Wong, M. S.Yang, R.Q. Zhang, S.T. Lee, Appl. Phys. Lett. 92 (2008) 043116.
[26] K.Q. Peng, X. Wang, S.T. Lee, Appl. Phys. Lett. 95 (2009) 243112.
[27] K.Q. Peng, X. Wang, X.L. Wu, S.T. Lee, Nano Lett. 9 (2009) 3704.
[28] K.Q. Peng, X. Wang, X.L. Wu, S.T. Lee, Appl. Phys. Lett. 95 (2009) 143119.
[29] W. Kern, D.A. Puotinen, RCA Rev. 31 (1970) 187.
[30] T. Qiu, P.K. Chu, Mater. Sci. Eng. R: Rep. 61 (1–6) (2008) 59.
[31] B. Zhao, H. Ma, Z. Zhang, et al., J. East. China Univ. Sci. Technol. 22 (2) (1996) 221.
[32] F. Zhao, G.A. Cheng, R.T. Zheng, L.Y. Xia, J. Korean Phys. Soc. 52 (2008) s104.
[33] S.J. Lee, A.R. Morrill, M. Moskovits, J. Am. Chem. Soc. 128 (2006) 2200.
[34] D.M. Lyons, K.M. Ryan, M.A. Morris, J.D. Holmes, Nano Lett. 2 (8) (2002) 811.
[35] V.A. Sivakov, G. Bronstrup, B. Pecz, A. Berger, G.Z. Radnoczi, M. Krause, S.H. Christiansen, J. Phys. Chem. C 114 (2010) 3798.